

Localized Dynamics in the Floquet Quantum East Model

Bruno Bertini^{1,2}, Pavel Kos³, and Tomaž Prosen⁴

¹*School of Physics and Astronomy, University of Nottingham, Nottingham, NG7 2RD, United Kingdom*

²*Centre for the Mathematics and Theoretical Physics of Quantum Non-Equilibrium Systems, University of Nottingham, Nottingham, NG7 2RD, United Kingdom*

³*Max-Planck-Institut für Quantenoptik, Hans-Kopfermann-Strasse 1, 85748 Garching, Germany*

⁴*Department of Physics, Faculty of Mathematics and Physics, University of Ljubljana, Jadranska 19, SI-1000 Ljubljana, Slovenia*

 (Received 6 July 2023; accepted 23 January 2024; published 22 February 2024)

We introduce and study the discrete-time version of the quantum East model, an interacting quantum spin chain inspired by simple kinetically constrained models of classical glasses. Previous work has established that its continuous-time counterpart displays a disorder-free localization transition signaled by the appearance of an exponentially large (in the volume) family of nonthermal, localized eigenstates. Here we combine analytical and numerical approaches to show that (i) the transition persists for discrete times, in fact, it is present for any finite value of the time step apart from a zero measure set; (ii) it is directly detected by following the nonequilibrium dynamics of the fully polarized state. Our findings imply that the transition is currently observable in state-of-the-art platforms for digital quantum simulation.

DOI: [10.1103/PhysRevLett.132.080401](https://doi.org/10.1103/PhysRevLett.132.080401)

Introduction.—Establishing the precise conditions for real space localization in interacting systems, even in one dimension, turns out to be extremely challenging. Despite intense efforts to crack it [1–9], it currently remains a major unsolved problem in theoretical physics. It has been argued that a form of many-body localization should emerge as a consequence of an external quenched disorder, which, under some conditions, might defeat interactions. Whether this mechanism can lead to a stable phase of matter remains an actively debated topic [7–9]. A fundamental problem is that localization studies are either limited to small systems accessible to numerical or experimental simulation or uncontrolled perturbative approximations. Nevertheless, for many-body localization to be established as a phase of matter, it has to exist in the thermodynamic limit: it should not (only) be a property of eigenstates, but (also) of dynamics.

Recently, it has been suggested that, other than by disorder, real space localization can also be triggered by kinetic constraints which render transport a higher-order process. An advantage of this approach is its immunity to fluctuating rare events such as ergodic bubbles. A minimal example of this mechanism is realized in the so-called quantum East model [10–15] (and its bosonic version [16]) where a localization transition in the quantum Hamiltonian

is in one-to-one correspondence with a first-order activity-inactivity transition in the corresponding classical stochastic glass model. In agreement with this picture, Ref. [17] observed an eigenstate localization transition in the quantum East model for an exponentially large family of eigenstates.

In this Letter, we take a fundamental step further and look for the possibility of dynamical localization in a Floquet, or Trotterized, version of the quantum East model, where localization is challenged by a steady pumping of energy into the system [18–20]. This setting can be seen as the kinetically constrained analog of Floquet many-body localization [21–23]. We replace the continuous Hamiltonian dynamics by a discrete sequence of conditional unitary gate operations—a quantum circuit—that can be conveniently implemented on platforms for digital quantum simulation, such as trapped ions [24–27] and superconducting circuits [28–33]. Using time-dependent perturbation theory, we argue that the model displays a localization transition by tuning the parameters of the model. We demonstrate that in the dynamically localized phase the model can be efficiently simulated by time-dependent matrix product methods [i.e., time-evolving block decimation (TEBD) algorithm] [34–36] to an arbitrary precision, showing very good quantitative agreement with the perturbative prediction. Moreover, we find qualitative agreement between the dynamical picture of localization in the infinite system and the localization of eigenstates in the finite system.

The model.—Our starting point is the quantum East model [10] defined by the following Hamiltonian operator (in arbitrary energy units):

Published by the American Physical Society under the terms of the Creative Commons Attribution 4.0 International license. Further distribution of this work must maintain attribution to the author(s) and the published article's title, journal citation, and DOI.

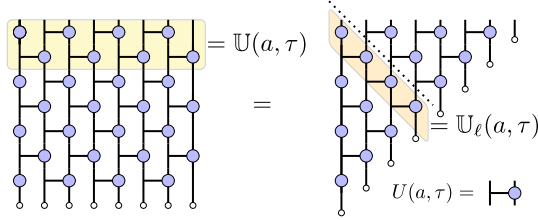


FIG. 1. Left: state (5) after $t = 3.5$ time steps of discrete dynamics. White bullets denote the state $|\downarrow\rangle$ and the blue circles the activation part of the conditional gate $U(a, \tau)$. The brick-wall Floquet propagator $\mathbb{U}(a, \tau)$ is highlighted in yellow. Right: explicit simplification of the dynamics out of the light cone. Dashed lines indicate the cut for the ladder evolution in Eq. (7). The ladder propagator $\mathbb{U}_\ell(a, \tau)$ [cf. (8)] is highlighted in orange.

$$H(a) = \sum_{j=1}^{2L-1} P_j(aX_{j+1} - I) + aX_1 - I. \quad (1)$$

Here a is the dimensionless coupling constant, $2L$ is the system size, $\{X_j, Y_j, Z_j\}$ are Pauli matrices acting nontrivially at site j , I is the identity operator, and $P_j = (I + Z_j)/2$.

We are interested in discrete sequences of unitary operations $\mathbb{U}(a, \tau)$ that reproduce the dynamics generated by Eq. (1) in a special scaling limit. Namely,

$$\lim_{t \rightarrow \infty} \mathbb{U}(a, t/t)^t = e^{-iH(a)t}, \quad (2)$$

where t is the number of discrete time steps, while t plays the role of physical time. This procedure is known as Trotter-Suzuki decomposition [37,38] and does not uniquely specify the unitary operator: there are many choices of $\mathbb{U}(a, \tau)$ fulfilling Eq. (2). Here we consider one that is local in space, i.e., it has the following brickwork structure (see Fig. 1):

$$\mathbb{U}(a, \tau) = e^{i\tau} \mathbb{U}_e(a, \tau) \mathbb{U}_o(a, \tau), \quad (3)$$

with

$$\begin{aligned} \mathbb{U}_e(a, \tau) &= U_{1,2}(a, \tau) \cdots U_{2L-1,2L}(a, \tau), \\ \mathbb{U}_o(a, \tau) &= e^{-i\tau a X_1} U_{2,3}(a, \tau) \cdots U_{2L-2,2L-1}(a, \tau), \end{aligned} \quad (4)$$

where we use a standard notation $O_{x,y}$ for an operator O acting nontrivially only at the sites x, y and define a local conditional gate $U(a, \tau) = e^{-i\tau(aP \otimes X - P \otimes I)}$. The (Trotter) time step τ , usually referred to as the Trotter step, sets the strength of the unitary operation (3). It is easy to verify that (2) holds for the evolution operator defined in Eq. (3). Note that the discrete-time dynamics generated by Eq. (3) is equivalent to a continuous-time dynamics in the presence of a periodic drive.

To probe the localization properties of the quantum circuit (3) we consider a ‘‘local quantum quench.’’ Namely, we prepare the circuit in the initial state

$$|\downarrow \cdots \downarrow\rangle, \quad (5)$$

which is an eigenstate of the bulk evolution due to the identity $U(a, \tau)|\downarrow\rangle = |\downarrow\rangle$, but is not stationary at the left boundary. As a consequence, only the sites within a light cone spreading from the left boundary undergo a nontrivial evolution, see Fig. 1. Intuitively, one can think of our local quench protocol as creating a localized disturbance in $(x, t) = (0, 0)$ in a state that is otherwise stationary. Importantly, this quench problem is also a caricature of local-operator spreading in a generic quantum many-body system after an operator-to-state mapping. Here, $|\downarrow\rangle$ [and (5)] represents the identity and $|\uparrow\rangle$ stands for any other traceless local operator that starts growing from the left edge. The question of localization now translates to that of the existence of a conserved local operator.

A simple measure of how the disturbance created by the local quench spreads through the system is given by the partial norms

$$W(x, t) = \sum_{s_j=\uparrow, \downarrow} |\langle s_1 \dots s_{x-1} \uparrow \downarrow \cdots \downarrow | \mathbb{U}(a, \tau)^t | \downarrow \cdots \downarrow \rangle|^2. \quad (6)$$

Since $W(x, t) \geq 0$ and $\sum_x W(x, t) = 1$, the partial norms can be thought of as the probability of having the rightmost up spin at position x . Specifically, whenever the disturbance remains localized at the boundary, we have $W(x, t) \approx 0$ for $x \gg x_0 = O(t^0)$, while when it spreads through the light cone the partial norms attain nonzero values for all $x \leq 2t$. We emphasize that due to the light cone $W(x > 2t, t) = 0$. The factor 2 is a direct consequence of the brickwork structure of (3), as each time step propagates information for up to two sites to the right.

In fact, to facilitate our numerical analysis we consider slightly modified quantities that bear the same physical information as those in Eq. (6): Instead of the partial norms of the state $\mathbb{U}(a, \tau)^t |\downarrow \cdots \downarrow\rangle$, we look at those of the state along the diagonal cut in the right panel of Fig. 1. The latter quantities are

$$N(x, t) = \sum_{s_j=\uparrow, \downarrow} |\langle s_1 \dots s_{x-1} \uparrow \downarrow \cdots \downarrow | \mathbb{U}_\ell(a, \tau)^t | \downarrow \cdots \downarrow \rangle|^2, \quad (7)$$

where we introduced the ‘‘ladder evolution operator’’ (cf. Fig. 1),

$$\mathbb{U}_\ell(a, \tau) = e^{i\tau} e^{-i\tau a X_1} U_{1,2}(a, \tau) U_{2,3}(a, \tau) \cdots U_{L-1,L}(a, \tau), \quad (8)$$

which is related to $\mathbb{U}(a, \tau)$ by a similarity transformation [39]. The quantities in Eq. (7) are more convenient than

those in Eq. (6) because with the same computational effort one can access times that are twice as long.

Infinite system at finite times.—Let us begin considering the time evolution of the partial norms $N(x, t)$ in the thermodynamic limit $L \rightarrow \infty$. In this case, the main qualitative features of their evolution can be understood by performing a simple perturbative analysis [the same can be done for $W(x, t)$, see the Supplemental Material [39]]. We begin by introducing the interaction representation of the time-evolution operator

$$\mathbb{U}_\ell(a, \tau)^t = \left[\prod_{k=0}^t \tilde{\mathbb{U}}_\ell(\tau a, \tau k) \right] e^{i\tau \sum_j P_j}, \quad (9)$$

where we defined

$$\tilde{\mathbb{U}}_\ell(a, \tau) = e^{i\tau} e^{-iaX_1} e^{-i\tau Z_1} \prod_{k \in \{1, \dots, 2L-1\}} \tilde{U}_{k, k+1}(a, \tau), \quad (10)$$

with $\tilde{U}(a, \tau) = e^{-iaP \otimes X} e^{-i\tau Z}$. We now fix x, t, τ and expand (6) in powers of a . Looking at the local gate in the interaction picture, i.e.,

$$\tilde{U}_{1,2}(a, \tau) = \mathbb{1} - iaP_1 X_2 e^{-i\tau Z_2} + O(a^2), \quad (11)$$

we have that $N(x)$ is at least of order a^{2x} . Indeed, due to the structure of Eq. (3), to get a spin up at position x we need to at least flip all the spins on its left. This also tells us

$$N(x, t) \simeq N'(x, t) \equiv \left| \langle \underbrace{\uparrow \cdots \uparrow}_x \downarrow \cdots \downarrow | \mathbb{U}(a, \tau)^t | \downarrow \cdots \downarrow \rangle \right|^2, \quad (12)$$

where \simeq denotes equality at the leading order in a . A simple combinatorial calculation then allows us to express it in terms of q -deformed binomial coefficients [39]

$$N(x, t) \simeq N'_1(x, t) \equiv (a\tau)^{2x} \left| \binom{t}{x}_q \right|^2, \quad (13)$$

where we set $q = e^{i\tau}$. Interestingly, the perturbative analysis commutes with the limit (2). Indeed, $\lim_{\tau \rightarrow 0} N'_1(x, t/\tau) = [2a \sin(t/2)]^{2x} / (x!)^2$, coincides with the leading order of (7) if one replaces (9) with its Trotter limit [39].

Let us now move on to analyze the localization properties of the perturbative solution. To this end, we assume that $N'_1(x, t)$ gives the only relevant contribution to the partial norm. The first key feature of $N'_1(x, t)$ is that its localization properties depend on whether or not τ is a rational multiple of 2π , namely, whether it can be written as $2\pi c/d$ for some coprime integers c and d . When true, the q -Lucas theorem [40] connects the behavior of q -deformed and regular binomials

$$\binom{t}{x}_q = \binom{\lfloor t/d \rfloor}{\lfloor x/d \rfloor} \binom{\text{mod}(t, d)}{\text{mod}(x, d)}_q, \quad (14)$$

where $\lfloor x \rfloor$ is the largest integer smaller than x and $\text{mod}(c, d)$ is the remainder of the division of $c \in \mathbb{N}$ by $d \in \mathbb{N}$. Using the Stirling approximation we find that Eq. (13) has a maximum at $\bar{x} = (a\tau)^{2d} t / [1 + (a\tau)^{2d}]$. Therefore, the support of $N'_1(x, t)$ grows in time, ruling out localization.

On the other hand, whenever τ is not a rational multiple of 2π , the deformed binomial coefficients are bounded in time. Namely, we have

$$\log \left| \binom{t}{x}_q \right|^2 = \sum_{p=1}^{t-x} \log \left[\frac{1 - \cos[\tau(x+p)]}{1 - \cos(\tau p)} \right] \simeq O(t^0). \quad (15)$$

In the last step, we used that, since $\{\text{mod}(\tau p, 2\pi)\}_{p=1}^t$ covers $[0, 2\pi)$ uniformly in the large t limit, we have

$$\sum_{p=1}^{t-x} \log(1 - \cos[\tau(y+p)]) \simeq (x-t) \log 2, \quad \forall y. \quad (16)$$

Therefore, the $O(t)$ in Eq. (15) cancels, and we are left with an $O(t^0)$ term. Plugging the bound Eq. (15) into Eq. (13), we find that $N'_1(x, t)$ is localized within a distance $x_0 = -1/(2 \log a\tau)$ from the left boundary for all times.

The second key feature is the τ dependence of a_c —the critical a for localization—in the case of irrational $\tau/(2\pi)$. In our setup, this amounts to asking for what range of a we expect the perturbative result to apply (at least qualitatively). From Eq. (13) we see that for finite τ the parameter that has to be small to ensure the validity of the perturbative approach is $a\tau$. Instead, in the limit $\tau \rightarrow 0$, the perturbative solution requires a itself to be small [39]. This suggests that a_c should be of the form

$$a_c(\tau) = \min(\alpha, \beta/\tau), \quad (17)$$

for some $\alpha, \beta \in \mathbb{R}$.

Remarkably, by computing $N(x, t)$ and $N'(x, t)$ via a simple version of the TEBD algorithm [39] we find that all these qualitative features persist away from the perturbative regime. Some representative examples of our numerical results are presented in Figs. 2 and 3, where, as a further indicator of localization, we also report the entanglement entropy $S(x, t)$ between the x leftmost sites and the rest of the system at time t .

For small enough a we see that disturbance created by the local quench remains localized only for irrational values of $\tau/(2\pi)$. This is clearly shown in the insets of Fig. 2: While for rational $\tau/(2\pi)$ we see the peak (and its position) of the entanglement entropy growing linearly in time, for

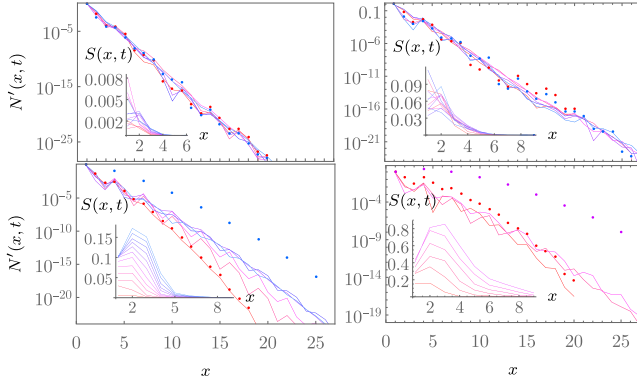


FIG. 2. Profiles of $N'(x, t)$ for $a = 0.1$ (left column), $a = 0.2$ (right column), and for $\tau = (\sqrt{5} - 1)\pi/2$ (top row), $\tau = 2\pi/3$ (bottom row). The data are shown for times $t = 20, 40, \dots, 120$ (red to blue curves), except for the bottom-right panel where only $t = 20, 40, 60$ can be computed due to fast growth of entanglement [insets indicate entanglement entropy profiles $S(x, t)$, $t = 10, 20, \dots$, of respective cases]. Colored bullets depict perturbative results for shortest and longest simulated time.

irrational $\tau/(2\pi)$ we see it saturating [additional corroborating plots of the (spatio)temporal behavior of $S(x, t)$, $W(x, t)$, and entanglement spectra are found in the Supplemental Material [39]]. Note that we observe this stark difference between rational and irrational $\tau/(2\pi)$ also for times that are significantly out of the perturbative regime ($t \gg 1/a$) and at which Eq. (13) is not quantitatively accurate: see the comparison in the main panel of Fig. 2. As a result of this localized behavior, for irrational $\tau/(2\pi)$ we are able to run our TEBD simulations with essentially no truncation error for hundreds of time steps.

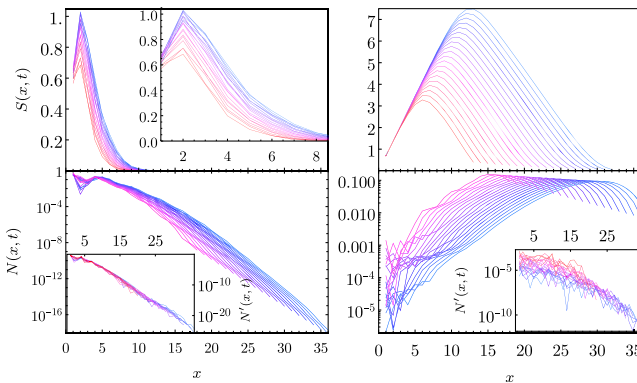


FIG. 3. Two cases of ergodic finite t and infinite size dynamics: left, right columns correspond, respectively, to $a = 0.3$, $\tau = (\sqrt{5} - 1)\pi/2$ just beyond localization transition and to $a = 1.0$, $\tau = (\sqrt{5} - 1)\pi/2$ well in the ergodic phase. We plot entanglement entropy profiles $S(x, t)$, partial norm profiles $N(x, t)$, and domain wall component profiles $N'(x, t)$ (insets) for $t = 17, 18, \dots, 36$ (red to blue).

On the other hand, for a larger than a certain critical value $a_c(\tau)$ the system transitions to the ergodic regime also for irrational $\tau/(2\pi)$, see Fig. 3. In this case, the perturbative result does not describe the system's behavior even at the qualitative level: the support of the partial norms grows linearly in time signaling a delocalization of the disturbance caused by the impurity. Concerning the τ dependence of $a_c(\tau)$, our numerical results are compatible with the functional form in Eq. (17) [39]. Namely, the critical a appears approximately τ independent for small τ , while it starts to decay as τ^{-1} when τ is increased beyond a threshold value.

Finite systems at infinite times.—Interestingly, the phenomenology observed above in the thermodynamic limit is also observed for finite volumes. Here we again look at a quench from the initial state in Eq. (5) but keep L finite while taking $t \rightarrow \infty$. A convenient indicator of the localization transition is then the time averaged square of the Loschmidt echo (LE) $|\langle \downarrow \cdots \downarrow | \mathbb{U}_\ell^s | \downarrow \cdots \downarrow \rangle|^2$ [this quantity is the same for brick-wall \mathbb{U} and ladder propagators \mathbb{U}_ℓ]. Assuming that there are no degeneracies in the spectrum of \mathbb{U}_ℓ , the LE can be written as $\lim_{t \rightarrow \infty} (1/t) \sum_s |\langle \downarrow \cdots \downarrow | \mathbb{U}_\ell^s(a, \tau) | \downarrow \cdots \downarrow \rangle|^2 = \sum_i |\langle \downarrow \cdots \downarrow | E_i \rangle|^4 \equiv I_{|\downarrow \cdots \downarrow \rangle}$, where the sum over i, j goes over all eigenstates. $I_{|\downarrow \cdots \downarrow \rangle}$ is the inverse participation ratio (IPR), which measures the spreading of the initial state in the eigenbasis of the time-evolution operator. It can be interpreted as the purity of the probability distribution $\{P_i\}$, with $P_i = |\langle \downarrow \cdots \downarrow | E_i \rangle|^2$ being the Born probability of measuring the eigenstate $|E_i\rangle$ in $|\downarrow \cdots \downarrow\rangle$. For random eigenstates $|E_i\rangle$, the probability distribution is flat, i.e., $P_i = 2^{-L}$, which gives $I_{|\downarrow \cdots \downarrow \rangle, \text{Haar}} = 2^{-L}$. In contrast, in the localized phase, we expect that, up to exponential corrections, the initial state spreads up to a finite distance k , so $\mathbb{U}^t |\downarrow \cdots \downarrow\rangle = |\psi\rangle |\downarrow \cdots \downarrow\rangle^{\otimes(L-k)}$, which leads to an IPR constant in L . Namely, $I_{|\downarrow \cdots \downarrow \rangle, \text{loc}} \geq 2^{-k}$ for all L .

We computed $I_{|\downarrow \cdots \downarrow \rangle}$ numerically for several values of a , τ , and L : our main numerical results are summarized in Fig. 4. The behavior of the IPR aligns remarkably well with the phenomenology of finite-time data. The bottom panel of the figure shows the IPR versus L for different values of a and three choices of τ . Identifying the localization transition as the transition between constant and exponentially decaying IPR, we can estimate $a_c(\tau)$. The last two τ are similar in size, but they are, respectively, irrational and rational multiples of 2π . We see that the difference between these two cases is stark also in this setting: the irrational $\tau/(2\pi)$ shows a transition at sizable a , while rational $\tau/(2\pi)$ shows ergodic behavior for the same choice of a . In the phase diagram, the rational $\tau/(2\pi)$ generate some irregular behavior reminiscent of Arnold tongues [41]. Some further discussion and additional finite-volume data are reported in the Supplemental Material [39].

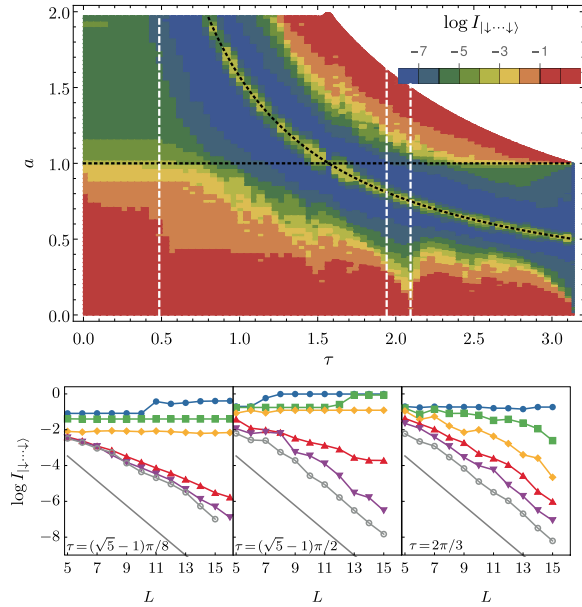


FIG. 4. Top: logarithm of the IPR at $L = 13$ as a function of τ and a . We see the transition for smaller (bigger) τ at $a = 1$ ($a \propto 1/\tau$). The dashed lines denote the three τ 's considered in the bottom panel. Bottom: logarithm of the IPR versus L for three values of τ and several values of a (0.5, 0.7, ..., 1.5 top to bottom for the first plot and 0.05, 0.15, ..., 0.55 for the second and third). The solid gray line corresponds to random eigenstates. For the first two τ 's the transition occurs around $a = 1$ and $a = 0.3$. The third τ is a rational multiple of 2π , and its transition occurs at a much smaller a . For a detailed analysis of this plot, see the Supplemental Material [39].

Discussion and outlook.—We introduced a discrete-time version of the quantum East model [10] and analyzed its localization properties in real time. Combining a perturbative analysis with exact numerics, we identified a localization transition taking place in this system despite the periodic drive: for couplings smaller than a critical value $a_c(\tau)$ the effect of a boundary perturbation remains localized in space, while it spreads ballistically for $a > a_c(\tau)$. This is also shown by a stark difference in the entanglement scaling (linear versus bounded), which is more marked than what is reported in other accounts of localization in Floquet settings [21,42]. Interestingly, this transition has a nonanalytic dependence on the Trotter time τ and takes place only when the latter is an irrational multiple of 2π . In fact, an irrational Trotter step and dynamical constraints can be identified as the two key mechanisms for the onset of localization. To understand this, one can imagine expanding the state of the system at time t in the computational basis. Because of the dynamical constraints, there will be far fewer states appearing in this sum than those allowed by the locality of the interactions. Moreover, all configurations are dampened by a factor $(\tau a)^x$, where x is the position of the up spin, that is further from the left boundary. This, however, is not enough to

ensure that the configurations with large x are suppressed—i.e., localization—because each configuration can be reached in many different ways, i.e., by many different “trajectories.” This means that, in the expansion of the state at time t , each configuration is multiplied by a “combinatorial weight,” which can, in principle, overcome the dampening. An irrational Trotter step avoids this by introducing destructive interference between the different trajectories, hence ensuring that the combinatorial weight never overcomes the exponential dampening. In the continuous time limit, $\tau \rightarrow 0$, the dampening factor goes to 0 and the combinatorial weight diverges; therefore, one has to combine the two effects. The outcome suggested by our analysis is that in this limit the system is localized for any $a < 1$, in agreement with Ref. [17]. This is not in contrast with the statement that the Floquet quantum East model is localized only for irrational $\tau/(2\pi)$, as in this case the limits of $\tau \rightarrow 0$ and $t \rightarrow \infty$ do not commute [43].

A natural question is what are the initial states for which localization occurs. We note that our analysis can be repeated for all states written as tensor products of arbitrary finite-block states with an infinite block of down spins on the right. This is consistent with the local-operator spreading analogy discussed earlier, as such states are those corresponding to local operators. States not fitting this form evade our treatment, leaving their analysis for future research. Our expectation is that those states will not show localization as in the continuous-time setting [17]. Indeed, they lack the first ingredient of the localization mechanism we identified, i.e., the presence of dynamical constraints. A key future direction is the rigorous characterization of the observed transition within the convenient discrete space-time setting introduced here.

P. K. thanks Giacomo Giudice for fruitful discussions. B. B. was supported by the Royal Society through the University Research Fellowship No. 201101. P. K. acknowledges financial support from the Alexander von Humboldt Foundation. T. P. acknowledges the Program P1-0402 and Grants No. N1-0219 and No. N1-0233 of the Slovenian Research and Innovation Agency (ARIS).

-
- [1] D. Basko, I. Aleiner, and B. Altshuler, Metal–insulator transition in a weakly interacting many-electron system with localized single-particle states, *Ann. Phys. (Amsterdam)* **321**, 1126 (2006).
 - [2] A. Pal and D. A. Huse, Many-body localization phase transition, *Phys. Rev. B* **82**, 174411 (2010).
 - [3] M. Serbyn, Z. Papić, and D. A. Abanin, Local conservation laws and the structure of the many-body localized states, *Phys. Rev. Lett.* **111**, 127201 (2013).
 - [4] V. Ros, M. Müller, and A. Scardicchio, Integrals of motion in the many-body localized phase, *Nucl. Phys.* **B891**, 420 (2015).

- [5] T. Thiery, F. Huveneers, M. Müller, and W. De Roeck, Many-body delocalization as a quantum avalanche, *Phys. Rev. Lett.* **121**, 140601 (2018).
- [6] D. A. Abanin, E. Altman, I. Bloch, and M. Serbyn, Colloquium: Many-body localization, thermalization, and entanglement, *Rev. Mod. Phys.* **91**, 021001 (2019).
- [7] J. Šuntajs, J. Bonča, T. Prosen, and L. Vidmar, Quantum chaos challenges many-body localization, *Phys. Rev. E* **102**, 062144 (2020).
- [8] D. Abanin, J. Bardarson, G. De Tomasi, S. Gopalakrishnan, V. Khemani, S. Parameswaran, F. Pollmann, A. Potter, M. Serbyn, and R. Vasseur, Distinguishing localization from chaos: Challenges in finite-size systems, *Ann. Phys. (Amsterdam)* **427**, 168415 (2021).
- [9] D. Sels and A. Polkovnikov, Dynamical obstruction to localization in a disordered spin chain, *Phys. Rev. E* **104**, 054105 (2021).
- [10] M. van Horssen, E. Levi, and J. P. Garrahan, Dynamics of many-body localization in a translation-invariant quantum glass model, *Phys. Rev. B* **92**, 100305(R) (2015).
- [11] P. Crowley, Entanglement and thermalization in many body quantum systems, Ph.D. thesis, University College London (UCL), 2017.
- [12] S. Roy and A. Lazarides, Strong ergodicity breaking due to local constraints in a quantum system, *Phys. Rev. Res.* **2**, 023159 (2020).
- [13] P. Brighi, M. Ljubotina, and M. Serbyn, Hilbert space fragmentation and slow dynamics in particle-conserving quantum East models, *SciPost Phys.* **15**, 093 (2023).
- [14] A. Geissler and J. P. Garrahan, Slow dynamics and non-ergodicity of the bosonic quantum East model in the semiclassical limit, *Phys. Rev. E* **108**, 034207 (2023).
- [15] K. Klobas, C. De Fazio, and J. P. Garrahan, Exact “hydrophobicity” in deterministic circuits: Dynamical fluctuations in the Floquet-East model, [arXiv:2305.07423](https://arxiv.org/abs/2305.07423).
- [16] R. J. Valencia-Tortora, N. Pancotti, and J. Marino, Kinetically constrained quantum dynamics in superconducting circuits, *PRX Quantum* **3**, 020346 (2022).
- [17] N. Pancotti, G. Giudice, J. I. Cirac, J. P. Garrahan, and M. C. Bañuls, Quantum East model: Localization, nonthermal eigenstates, and slow dynamics, *Phys. Rev. X* **10**, 021051 (2020).
- [18] A. Lazarides, A. Das, and R. Moessner, Equilibrium states of generic quantum systems subject to periodic driving, *Phys. Rev. E* **90**, 012110 (2014).
- [19] L. D’Alessio and M. Rigol, Long-time behavior of isolated periodically driven interacting lattice systems, *Phys. Rev. X* **4**, 041048 (2014).
- [20] P. Ponte, A. Chandran, Z. Papić, and D. A. Abanin, Periodically driven ergodic and many-body localized quantum systems, *Ann. Phys. (Amsterdam)* **353**, 196 (2015).
- [21] P. Ponte, Z. Papić, F. Huveneers, and D. A. Abanin, Many-body localization in periodically driven systems, *Phys. Rev. Lett.* **114**, 140401 (2015).
- [22] A. Lazarides, A. Das, and R. Moessner, Fate of many-body localization under periodic driving, *Phys. Rev. Lett.* **115**, 030402 (2015).
- [23] D. A. Abanin, W. De Roeck, and F. Huveneers, Theory of many-body localization in periodically driven systems, *Ann. Phys. (Amsterdam)* **372**, 1 (2016).
- [24] B. P. Lanyon, C. Hempel, D. Nigg, M. Müller, R. Gerritsma, F. Zähringer, P. Schindler, J. T. Barreiro, M. Rambach, G. Kirchmair *et al.*, Universal digital quantum simulation with trapped ions, *Science* **334**, 57 (2011).
- [25] J. T. Barreiro, M. Müller, P. Schindler, D. Nigg, T. Monz, M. Chwalla, M. Hennrich, C. F. Roos, P. Zoller, and R. Blatt, An open-system quantum simulator with trapped ions, *Nature (London)* **470**, 486 (2011).
- [26] R. Blatt and C. F. Roos, Quantum simulations with trapped ions, *Nat. Phys.* **8**, 277 (2012).
- [27] C. Monroe, W. C. Campbell, L.-M. Duan, Z.-X. Gong, A. V. Gorshkov, P. W. Hess, R. Islam, K. Kim, N. M. Linke, G. Pagano, P. Richerme, C. Senko, and N. Y. Yao, Programmable quantum simulations of spin systems with trapped ions, *Rev. Mod. Phys.* **93**, 025001 (2021).
- [28] Y. Salathé, M. Mondal, M. Oppliger, J. Heinsoo, P. Kurpiers, A. Potočnik, A. Mezzacapo, U. Las Heras, L. Lamata, E. Solano, S. Filipp, and A. Wallraff, Digital quantum simulation of spin models with circuit quantum electrodynamics, *Phys. Rev. X* **5**, 021027 (2015).
- [29] R. Barends, L. Lamata, J. Kelly, L. García-Álvarez, A. G. Fowler, A. Megrant, E. Jeffrey, T. C. White, D. Sank, J. Y. Mutus *et al.*, Digital quantum simulation of fermionic models with a superconducting circuit, *Nat. Commun.* **6**, 7654 (2015).
- [30] N. K. Langford, R. Sagastizabal, M. Kounalakis, C. Dickel, A. Bruno, F. Luthi, D. J. Thoen, A. Endo, and L. DiCarlo, Experimentally simulating the dynamics of quantum light and matter at deep-strong coupling, *Nat. Commun.* **8**, 1 (2017).
- [31] G. Wendin, Quantum information processing with superconducting circuits: A review, *Rep. Prog. Phys.* **80**, 106001 (2017).
- [32] M. Kjaergaard, M. E. Schwartz, J. Braumüller, P. Krantz, J. I.-J. Wang, S. Gustavsson, and W. D. Oliver, Superconducting qubits: Current state of play, *Annu. Rev. Condens. Matter Phys.* **11**, 369 (2020).
- [33] S. Bravyi, O. Dial, J. M. Gambetta, D. Gil, and Z. Nazario, The future of quantum computing with superconducting qubits, *J. Appl. Phys.* **132**, 160902 (2022).
- [34] G. Vidal, Efficient simulation of one-dimensional quantum many-body systems, *Phys. Rev. Lett.* **93**, 040502 (2004).
- [35] U. Schollwöck, The density-matrix renormalization group in the age of matrix product states, *Ann. Phys. (Amsterdam)* **326**, 96 (2011).
- [36] J. I. Cirac, D. Pérez-García, N. Schuch, and F. Verstraete, Matrix product states and projected entangled pair states: Concepts, symmetries, theorems, *Rev. Mod. Phys.* **93**, 045003 (2021).
- [37] M. Suzuki, General theory of fractal path integrals with applications to many-body theories and statistical physics, *J. Math. Phys. (N.Y.)* **32**, 400 (1991).
- [38] H. F. Trotter, On the product of semi-groups of operators, *Proc. Am. Math. Soc.* **10**, 545 (1959).
- [39] See Supplemental Material at <http://link.aps.org/supplemental/10.1103/PhysRevLett.132.080401> for (i) a combinatorial calculation of $N(x, t)$, (ii) a perturbative analysis of brickwork partial norms $W(x, t)$, (iii) a perturbative analysis of $N(x, t)$ in the Trotter limit, (iv) a self-contained discussion of our TEBD algorithm, (v) further

TEBD data, (vi) comparison of ladder and brick-wall settings, (vii) detailed analysis of Fig. 4, and (viii) further finite-volume data.

- [40] B. E. Sagan, Congruence properties of q -analogs, *Adv. Math.* **95**, 127 (1992).
- [41] V. I. Arnold, Small denominators. I. Mapping the circle onto itself, *Izv. Akad. Nauk SSSR Ser. Mat* **25**, 21 (1961).
- [42] S. Ray, S. Sinha, and K. Sengupta, Signature of chaos and delocalization in a periodically driven many-body system: An out-of-time-order-correlation study, *Phys. Rev. A* **98**, 053631 (2018).
- [43] To see this, we observe that to get to $\tau = 0$ using rational multiples of 2π one has to take $\tau = 2\pi/d$ with increasingly large $d \in \mathbb{N}$. In this case, delocalization is expected to emerge only for $t \gg d$ [cf. (14)], leading to the claim.